Pure and Applied Geophysics

CrossMark

Thermodynamics and Microphysics Relation During CAIPEEX-I

SUDARSAN BERA,[1] 🔘 T. V. PRABHA,[1] N. MALAP,[1] S. PATADE,[2] M. KONWAR,[1] P. MURUGAVEL,[1] and D. AXISA[3]

Abstract—Influence of the environmental thermodynamics on the microphysics of deep cumulus clouds over different parts of India is studied using in situ airborne observations from the Cloud Aerosol Interaction and Precipitation Enhancement EXperiment (CAIPEEX) during 2009. This study provides an understanding of the thermodynamics–microphysics relation over the Indian summer-monsoon region. Relatively stronger updraft and turbulence are noted in the pre-monsoon cloud base layers compared to that of the monsoon clouds. It is illustrated from the in situ observations as well as from a microphysical parcel model that the vertical variation of cloud droplet number concentration (CDNC) has a well-defined peak at a certain height above the cloud base. This elevated CDNC peak is found to be connected with the cloud parcel buoyancy and cumulative convective available potential energy (cCAPE). Higher parcel buoyancy above the cloud base of dry pre-monsoon clouds is associated with stronger in-cloud updraft velocity, higher supersaturation and higher droplet number concentration (in addition to aerosol effect). Higher adiabatic fraction and lower entrainment rate are observed in polluted clouds where boundary layer moisture is low, compared to clean clouds. Relative dispersion of droplet size distribution is found to vary concurrently with air mass characteristics and aerosol number concentration observed over different locations during the experiment. Aerosol–precipitation relationships are also investigated from the observation. Maximum reflectivity and rain rates showed a direct link with boundary layer water vapor content rather than with subcloud aerosol number concentration.

1. Introduction

Cumulus clouds are widely prevalent and considered to be a key controller of global water cycle and radiation budget (Warren et al. 1986; Siebesma et al. 2003; Morrison and Grabowski 2007). Due to their importance to global climate, it is required to examine various factors that affect the microphysics

of cumulus clouds. Increasing aerosol pollution for a fixed amount of water vapor produces smaller cloud droplets with higher number concentration and brightens the clouds. This leads to reflection of more shortwave radiation back to the space and increases the life time of the clouds by suppressing collision–coalescence of droplets which is known as second indirect effect (Twomey 1977; Albrecht 1989; Wang et al. 2003; Ackerman et al. 2004; Xue and Feingold 2006). The variation of aerosol concentration is usually associated with the thermodynamic change of the atmosphere and both (aerosol and thermodynamics) are connected with cloud microphysics (Khain et al. 2005; Mechem et al. 2012; Gayatri et al. 2017). An extensive investigation of aerosol effects on precipitation is given by Khain (2009). Over several instances, aerosol is suggested to invigorate convection and increase precipitation (Rosenfeld et al. 2008; Fan et al. 2018). But whether the invigoration is caused by dynamical or microphysical effect (Li et al. 2011) is still difficult to establish from observations due to the non-linear interactions between the microphysical and dynamical effects.

Over the Indian subcontinent, warm and dry environment (e.g., pre-monsoon) is accompanied by higher aerosol number concentration but relatively cold and wet environment (e.g., monsoon) is associated with low aerosol number concentration (Prabha et al. 2011). Konwar et al. (2012) showed that droplet growth in warm cloud is suppressed under high aerosol condition and aerosol loading can increase the height of warm rain initiation. However, in certain conditions, the suppression of rain formation in the warm region of the cloud has resulted in precipitation from a mixed phase region (Patade et al. 2015).

During the onset of summer monsoon over Indian land mass, boundary layer thermodynamics changes

[1] Indian Institute of Tropical Meteorology, Pune, India. E-mail: sbera.cat@tropmet.res.in
[2] Department of Physical Geography and Ecosystem Science, Lund University, Lund, Sweden.
[3] Droplet Measurement Technologies, Longmont, USA.

rapidly in association with change in aerosol number concentration (Prabha et al. 2011; Bera et al. 2016b). The microphysics of deep cumulus clouds during pre-monsoon and monsoon over India was studied in many previous studies (Prabha et al. 2011, 2012; Bera et al. 2016a; Konwar et al. 2012) but a detailed understanding of thermodynamics–microphysics interaction from these datasets was lacking. The present study addresses this issue with a main objective to understand the thermodynamics–microphysics interaction over the monsoon region.

Droplet size distribution (DSD) and associated microphysics of raindrop formation mechanism have been studied extensively by many research groups, but they mostly focused on the marine stratocumulus/shallow cumulus clouds (Warner 1969; Jensen and Baker 1989; Tölle and Krueger 2014). Miles et al. (2000) gave a comprehensive list of droplet dispersion in marine and continental clouds, but observations in the continental cumulus/deep convective clouds are seldom available, except for a few cases from Gulf of Mexico Atmospheric Composition and Climate Study (GoMACCS) (Lu et al. 2008) and the Large-Scale Biosphere–Atmosphere Experiment in Amazonia–Smoke, Aerosols, Clouds, Rainfall, and Climate (BLA-SMOCC) (Andrea et al. 2004). Pandithurai et al. (2012) investigated the indirect effect and dispersion effect in these clouds (using CAIPEEX observations) and found that dispersion effect may offset the indirect effect depending on the degree of adiabaticity. Droplet spectral dispersion characteristics of pre-monsoon and monsoon clouds in highly polluted regions under both dry and wet conditions showed distinct vertical variations (Prabha et al. 2012). However, a comprehensive idea on the vertical variation of microphysical characteristics of clouds observed during CAIPEEX in relation to the adiabatic parcel properties is still unestablished. In a campaign such as CAIPEEX 2009, it was nearly impossible to have similar thermodynamic conditions while the observational site moved from place to place as monsoon progressed over inland areas. The main aim of CAIPEEX 2009 was to get samples of aerosol and cloud observations as monsoon onset took place at different continental locations. Survey flights were conducted for collecting first time cloud microphysical data in developing clouds with an intention to look for the possibility of weather modification prospects. It is important to document the thermodynamical changes along with the microphysical changes and aerosol observations.

The droplet size distribution (DSD) is strongly dependent on the activation/evaporation and collision–coalescence processes which eventually lead to the growth/dissipation of the clouds. The thermodynamics of the environment also impacts the cloud microphysics through entrainment of droplet free dry air into the cloud, and influencing the activation/evaporation of droplets (Bera et al. 2016b). Depending on the characteristics of the entrained air, the droplet size spectrum (DSD) may change and impact the surrounding environment also (Jensen et al. 1985; Tölle and Krueger 2014).

Over the Indian region, the pre-monsoon and monsoon conditions and the transition like situation have significantly different thermodynamic characteristics (Prabha et al. 2011; Kulkarni et al. 2012; Bera et al. 2016b; Thomas et al. 2018). The cloud base during the pre-monsoon is at higher altitude (deeper boundary layer) with clouds having small droplet size and higher number concentration due to high aerosol condition. In the monsoon case, the cloud base is at a lower altitude and droplet number concentration is low with larger droplet size. The droplet spectral characteristics have been explored extensively from the CAIPEEX observations (Kulkarni et al. 2012; Prabha et al. 2012; Bera et al. 2016a). However, the signature of the thermodynamics on the cloud microphysical changes has not been explored. The present study is an attempt to relate the thermodynamical and microphysical characteristics from CAIPEEX 2009 experiment, in which the observational base station was moved according to the progression of monsoon and the availability of the clouds.

2. Data and Methods

Cloud Aerosol Interaction and Precipitation Enhancement EXperiment (CAIPEEX) was the first airborne campaign in India, focusing on the microphysics of pre-monsoon and monsoon clouds. An instrumented research aircraft was used to document

the various properties of aerosol and cloud micro-physics. Details of the experiment, data and instruments were reported in several previous studies (Prabha et al. 2011; Kulkarni et al. 2012; Nair et al. 2012) and also available at the web page http://www.tropmet.res.in/~caipeex/.

In the present study, we used data from the CAIPEEX phase-I conducted during May–September, 2009. Observations over several places in India (indicated in Fig. 1) are focused in characterization of different types of clouds and their microphysical structure. Observations of deep convective clouds (mostly continental cumulus-congestus) up to 6 km above cloud base were carried out during the experiment. These are unique observations in the aerosol laden tropical land area. Few observations over the coastal areas are also presented.

The instruments used in Phase-I of CAIPEEX are described in Table 1. The SOAR Piper Cheyenne II research aircraft was equipped with a Passive Cavity Aerosol Spectrometer Probe (PCASP-SPP-200) which measures the aerosol particles in the diameter range 0.1–3.0 μm and a Cloud Droplet Probe (CDP) to measure concentration and droplet size distribution (DSD) in the size range 2–50 μm. DMT cloud imaging probe (CIP) was used for measurement of cloud particles in the size range 25–1550 μm. Liquid water content (LWC) was measured by a hot wire

Figure 1

CAIPEEX Phase-I flight tracks over different parts of India. Dates mentioned on the figure correspond to the year 2009

maintained at a constant temperature. Humidity, temperature and winds are measured by Aircraft Integrated Meteorological Measurement System (AIMMS) probe. Sampling intervals used for each of the instruments were 1 Hz.

The areas of cloud sampling were identified based on maximum liquid water content inside the cloud. Sampling area of 25 km × 25 km around the maximum LWC region is used in estimating the in-cloud parameters. Subcloud parameters are averaged for 50 km × 50 km area around the identified cloud based on maximum LWC. The cloud base droplet number concentration, LWC, spectral width, mean radius and relative dispersion are estimated (averaged) for the non-precipitating regions of clouds within the 1 km above the cloud base. The vertical variations of various parameters are presented using cloud pass data averaged at each 200 m height level above cloud base. The standard deviation of data at each level was also calculated and presented by error bars. The standard deviation at a specific level represents the spatial fluctuations of the parameter along the cloud pass. The in-cloud samples are detected by filtering the data points with 10 cm^{-3} droplet number concentration (CDNC > 10 cm^{-3}) thresholds (Rangno and Hobbs, 2005).

The aerosol and hence CCN concentration has significant variation from pre-monsoon (April and May) to monsoon season (June, July, August, September). During the pre-monsoon and monsoon periods, considerable variability in the dynamic and thermodynamic properties of the atmosphere is observed across the Indian subcontinent. Precipitable water was found to be a good proxy to define the Lifting Condensation Level (LCL) over the continental area (Murugavel et al. 2017). The cloud droplet probe (CDP) and cloud imaging probe (CIP) jointly provide the combined cloud-raindrop size distribution in the diameter range from 2.5 to 1550 μm. The CDP is used to derive droplet spectral characteristics. The drop size distribution from CIP has been processed to derive few parameters such as reflectivity and rain rate. Rain rate is determined from particle fall velocity, liquid water content, and number density. Reflectivity is derived using the sixth power of particle size (maximum diameter).
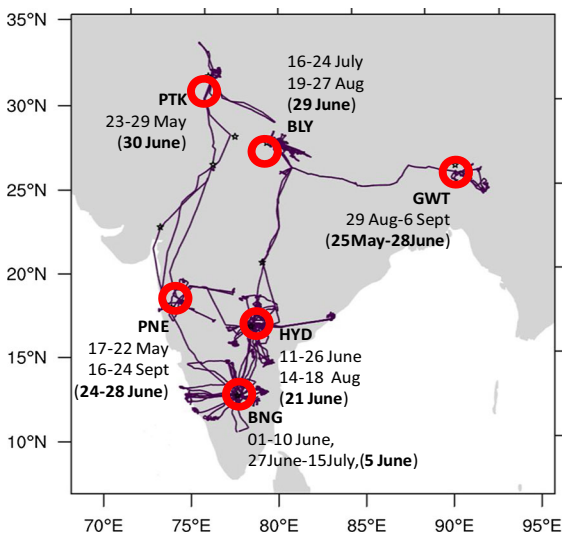
Table 1

Table with details of instruments, range, resolution and frequency

Instruments	Measurement description	Range	Resolution	Frequency
Rosemount temperature	Air temperature	− 50 °C to + 50 °C	0.01 °C	1 Hz
GPS sensor	Latitude	–	< 1 m	5 Hz
	Longitude	–	< 1 m	5 Hz
	Altitude	− 300 to 18,000 m	< 1 m	5 Hz
AIMMS-20 probe	Air temperature, relative humidity, pressure, and three-dimensional wind components	− 30 °C to + 50 °C	0.01 °C	< 1 s TC
		0–100%	0.1% RH	5 s TC @
		0–110,000 Pa	10 Pa	20 °C
		–	0.5 m s^{-1} @ 75 m s^{-1} TAS	20 Hz
				5 Hz
DMT CDP	Cloud droplet spectra and number concentration	2–47 μm	1–2 μm 30 bins	1 Hz
DMT CIP	Small precipitation particle size, concentration, and shape	25–1550 μm	25 μm, 62 bins	1 Hz
DMT LWC-100	Liquid water content (SAWS)	0–3.0 g m^{-3}	0.01 g m^{-3}	1 Hz
DMT CCN counter	Cloud condensation nuclei concentration and spectra (WITS	0.5–10 μm @ 0.1–1.2% SS	0.5 μm, 20 bins	1 Hz
DMT SPP-200 (PCASP)	Aerosol concentration and size spectra	0.1–3.0 μm	0.02 μm, 30 bins	1 Hz

The radiosonde observations were taken at 11:00 IST (local time), before the flight observations and utilized for deriving environmental parameters such as precipitable water (PW), convective available potential energy (CAPE) and lifting condensation level height (LCL) and corresponding temperature (T_{LCL}). The flight observations started during very dry conditions (May–June) with precipitable water (PW) below 3 cm and often exceeded 6 cm when south–west monsoon set up over the subcontinent. In general, CAPE is reduced and LCL height is lowered with the establishment of monsoon conditions.

The fractional entrainment rate used in this study is estimated by following the same methodology as used in Lu et al. (2012) and details of application using CAIPEEX data are also provided in Bera et al. (2016a). This methodology uses the concept of mass fraction of cloudy volume at different heights above the cloud base. The mass fraction at a height (*h*) above the cloud base is the ratio of adiabatic cloud mass at the cloud base to the total mass (cloudy volume + entrained air) after mixing at height *h* above the cloud base.

3. Results

The main emphasis of the study is to investigate the relationship between the environmental thermodynamics and the cloud microphysics in association with aerosol variation, observed during the entire period of CAIPEEX-I (mainly because CAIPEEX-I observations covered the entire monsoon season at different locations of India). It is noted that droplet spectra in supercontinental dry condition were narrow with much less variation in the spectral width and mean radius with height (Prabha et al. 2012). Recently, some studies illustrated that increasing aerosols can decrease precipitation in the dry environment, while in the moist environment, total precipitation and precipitation intensity may increase by aerosol pollution (Gayatri et al. 2017). However, the role of thermodynamic condition (other than aerosol effect) also needed to be investigated to link it up with the microphysics. Thermodynamic observations, illustrated here are from the radiosonde soundings (RS-80).
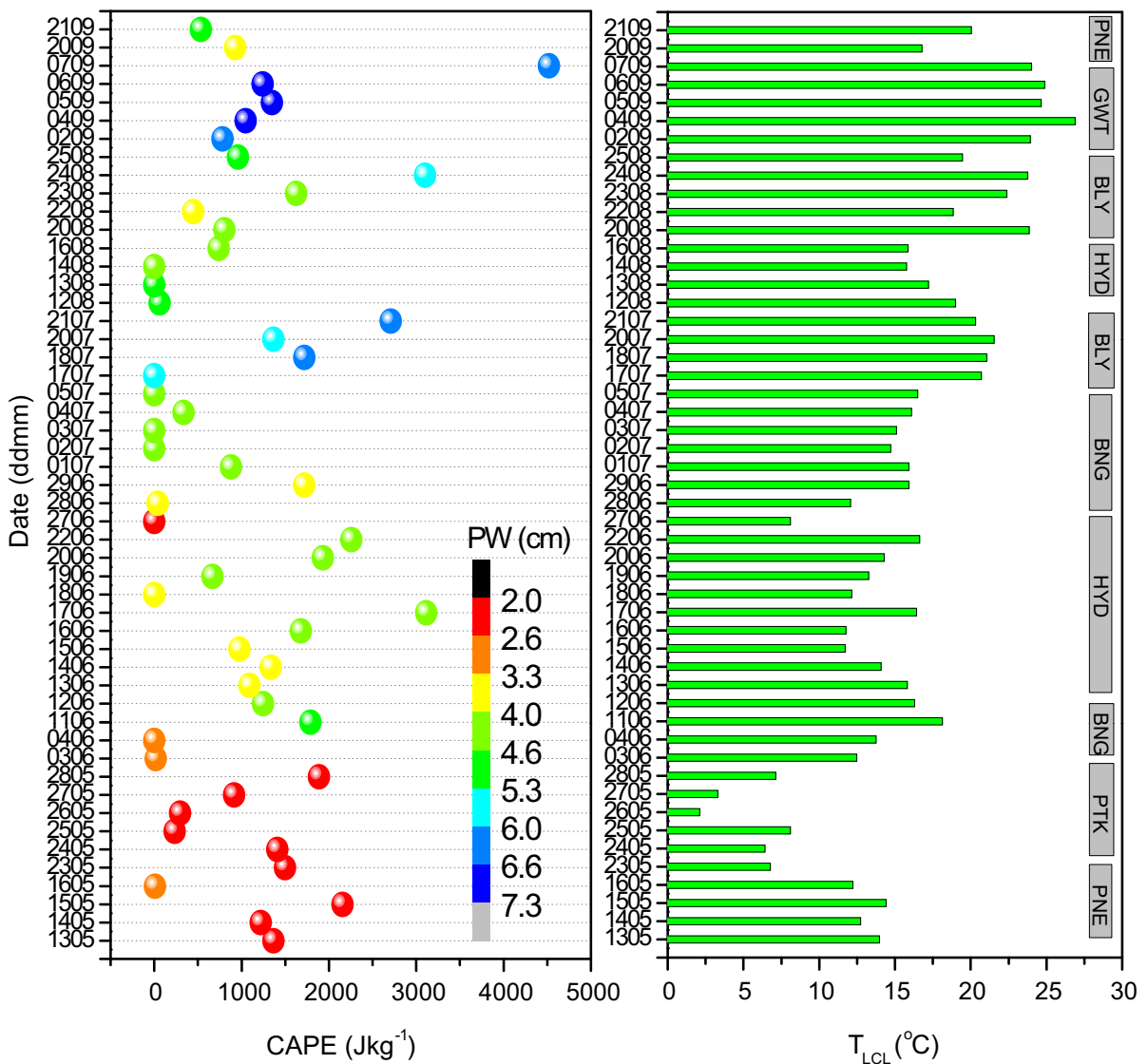
Figure 2
a Variation of convective available potential energy (CAPE, J kg^{-1}), Precipitable Water (PW, cm in color) with the dates (ddmm; dd for day and mm for month) and **b** LCL temperature (T_{LCL}) over various locations (from radiosonde observation) as indicated on vertical boxes (right side)

3.1. Thermodynamic Parameters

Figure 2 gives an overview of the estimated CAPE, integrated water vapor (PW) and LCL temperature from the radiosonde observations conducted during the campaign routinely from the base stations as indicated in Fig. 1 (dates of observations are also indicated). CAPE was significantly high in the beginning of the study period (pre-monsoon) and it

is interesting that high CAPE was also noted at other locations as monsoon progressed. A few of those high CAPE cases have high PW towards the end of the experiment (as indicated with color in Fig. 2a). LCL temperature variation is presented in Fig. 2b. All cases have warm (above 0 °C) LCL temperature and only during the pre-monsoon period (23/05/2009 to 28/05/2009) over Pathankot (PTK) has lowest LCL

temperature below 5 °C. We mostly targeted clouds with warm bases and registered liquid water content.

In summary: CAPE exceeded 2000 J kg^{-1} during the pre-monsoon and the initial monsoon periods. As the monsoon progressed, the CAPE was reduced, LCL height was reduced and PW was increased. However, few cases in monsoon environment also have very high CAPE (exceeding 2000 J kg^{-1}) but overall monsoon cases have lower CAPE which is due to reduced solar insolation in cloudy monsoon environment.

3.2. Cloud Top, Cloud Base and Cloud Depth

The variation of cloud base height, cloud top height and cloud depth derived from research flight observations at various locations are shown in Fig. 3a. BNG; Bangalore and BLY; Bareilly characterized deepest clouds. While in most cases, cloud depth was more than 3 km, indicating deep convective clouds/deep cumulus. The relationship between cloud depth and liquid water path (LWP), derived from aircraft observations is shown in Fig. 3b which indicates high LWP corresponds to deeper clouds and vice versa. The relations of cloud depth with precipitable water and LCL temperature (T_{LCL}) which are derived from radiosonde soundings
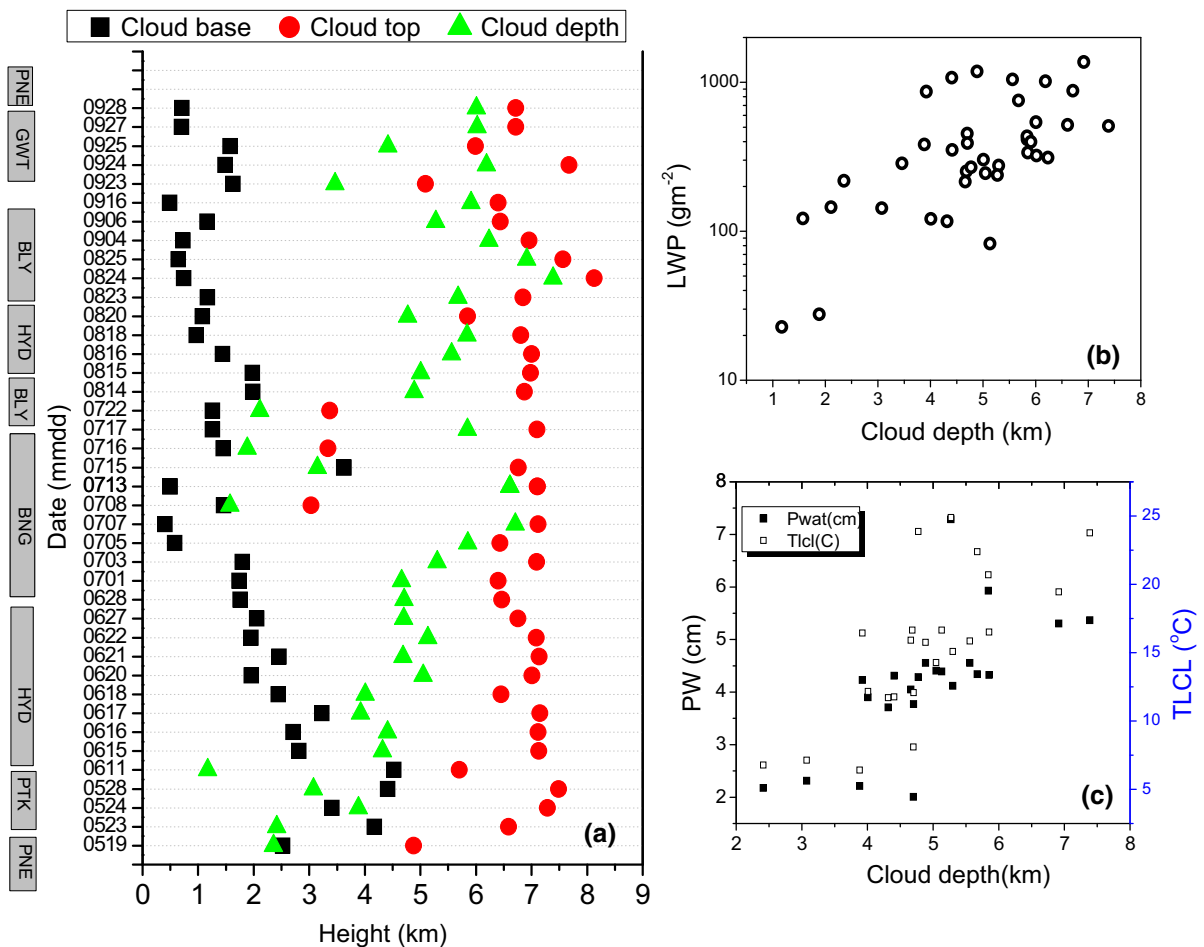

Figure 3
a Variation of cloud base, cloud top and cloud depth derived from flight observations at various locations, **b** the relationship between Cloud depth and LWP and **c** relationship between the cloud depth and precipitable water/LCL temperature derived from radiosonde observations
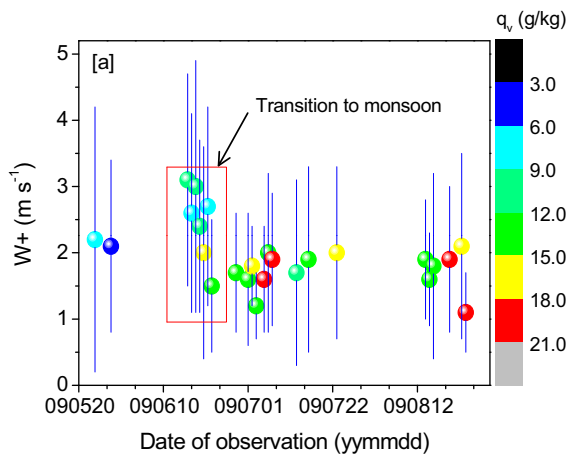
Figure 4

Variation of mean updraft velocity (up to 1 km above cloud base) during pre-monsoon and monsoon periods. Averaged water vapor mixing ratio of boundary layer is presented by the color code

(Fig. 3c) also show a nearly linear dependence on each other. High PW coincided with lower cloud base heights and higher cloud depth. Cloud depth and LWP are positively correlated (Fig. 3b) as higher cloud depth is associated with higher liquid water content (LWC). Similarly, cloud depth is also positively related to PW and LCL temperature. Cloud base height is decreased after the establishment of monsoon with sufficient low level moisture, which resulted in an increased cloud depth and LWP. Cloud top height of the observed cumulus-congestus is more or less constant (except for a few cases) and is about 7–8 km mainly due to the inversions layer above these height levels.

3.3. Updrafts Above Cloud Base

Figure 4 shows the mean updrafts (incloud) within 1 km above cloud base derived from the aircraft AIMMS probe observations. Data show that mean updrafts inside the clouds vary with time as monsoon progresses. Spatial variation of observation is given by error bars. One important aspect is that updrafts are stronger during the pre-monsoon and the transition to monsoon. These strong updrafts in the cloud base region are important for microphysical characterization and have been investigated in the present study. It is observed that pre-monsoon strong updrafts are associated with higher buoyancy and

CAPE and that indicate likelihood of high supersaturation. The activation of additional droplets above the cloud base is supported by these higher updrafts strength.

3.4. Relationship Between Entrainment Parameters and Boundary Layer Water Vapor

In this section, we have used the adiabatic fraction, the ratio of cloud liquid water content (measured from aircraft observation; CDP probe) to adiabatic liquid water content in the clouds (as predicted by adiabatic parcel model). Adiabatic fraction gives an idea on the adiabaticity of the clouds. A value equal to 1.0 indicates that cloud is fully adiabatic and any other values less than 1.0 indicate that dry air is entraining into the cloud and the cloud is diluted.

Since there is a clear indication that cloud depth is controlled by the availability of water vapor content (or PW) in the atmosphere, here we investigate the role of boundary layer water vapor content in dictating the dilution of convective clouds by the process of entrainment-mixing. Results are presented in Fig. 5a with a scatter plot showing the relationship between boundary layer water vapor and adiabatic fraction. This shows that under highly moist conditions, clouds are more diluted and in dry conditions they are more adiabatic. There are some exceptions to these effects for clouds growing in highly polluted moist environment (not presented). In general, polluted clouds are associated with drier environment and have higher adiabatic fraction. Bera, Pandithurai, et al. (2016) showed that polluted clouds have strong adiabatic core which is not affected by dry air entrainment. But less polluted monsoon clouds have lower droplet number concentration and they are less adiabatic in the core region. However, it may be noted that these results are consistent for the entire cloud observations and have a linear (negative) relation with the water vapor content in the boundary layer. A strong negative correlation (-0.87) between water vapor mixing ratio in the boundary layer and adiabatic fraction (Fig. 5a) is revealed from our observations. This kind of analysis was possible due to the varying thermodynamic conditions (such as PW) available with the observations. High adiabatic
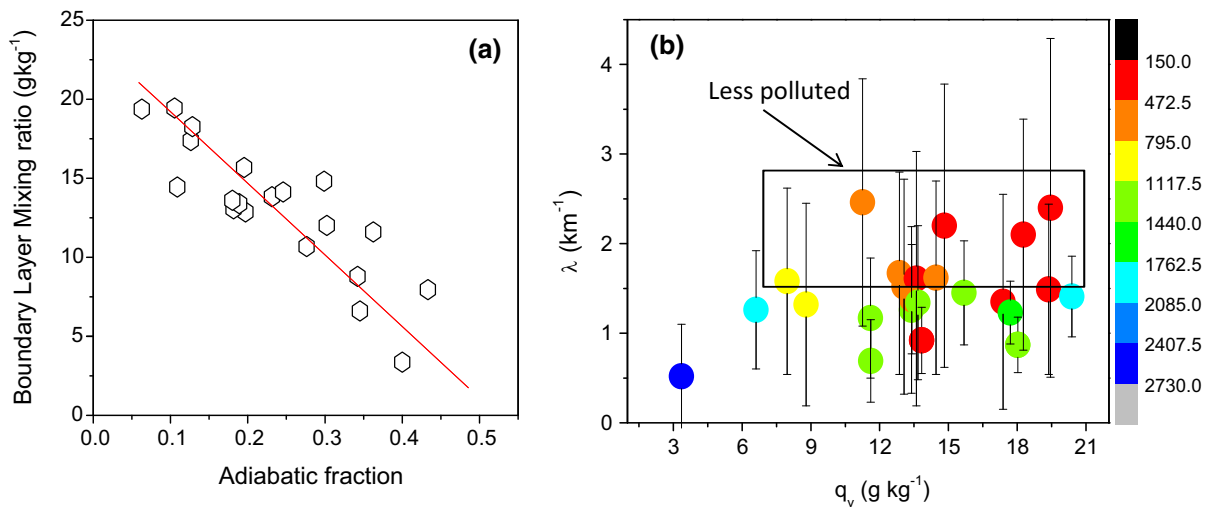
Figure 5
Correlation of adiabatic fraction and water vapor mixing ratio (**a**), Variation of mean entrainment rate (up to 2 km above cloud base) with boundary layer water vapor mixing ratio (**b**). Color scale in **b** is aerosol number concentration (cm^{-3})

fraction is also associated with high droplet and aerosol number concentration values. This is due to the fact that dry conditions are also more polluted and number concentration of aerosols is higher compared to the moist conditions.

In general, cumulus clouds are significantly diluted due to dry air entrainment from cloud top or from lateral cloud boundary (Paluch 1979; Blyth et al. 1988; Raga et al. 1990; Gerber et al. 2008; Böing et al. 2014). We emphasize on the role of environmental thermodynamics on dry air entrainment strength. Fractional entrainment rate averaged for 2 km depth above cloud base is presented in Fig. 5b. Fractional entrainment rate varied with boundary layer water vapor mixing ratio and no clear correlation is observed, unlike the case of adiabatic fraction which also provides information of lateral entrainment effect. However, Fractional entrainment rate is poorly correlated with aerosol number concentration which shows that less polluted monsoon clouds have higher entrainment rate which may dilute clouds more, as illustrated by the adiabatic fraction. This indicates that lateral entrainment is quite important for monsoon clouds and is to be accounted for in the numerical weather prediction (NWP) models. The cumulus-congestus or deep cumulus clouds probed during CAIPEEX are constantly entrained by the action of strong wind shear which is a general feature of monsoon.

3.5. Impact on Microphysical Parameters and Aerosol–Precipitation Relations

To investigate further the thermodynamics–aerosol–microphysics linkage in monsoon environment, we consider the boundary layer v component wind velocity as an indicator for the continental or maritime air mass origin. During the monsoon, strong positive v component is associated with southwesterly wind (monsoon low-level jet, LLJ) that transports moisture from the Arabian Sea to inland. The modification of air mass characteristics during dry condition (break spell) occurs mainly due to the northern continental air intrusion (negative v component) which is associated with higher aerosol concentration. This may be noted from the mean boundary layer aerosol concentration and droplet number concentration showing a strong relationship with v velocity (shown in Fig. 6a). All incloud parameters are estimated for the cloud passes near to the cloud base and are averaged within 1 km above the cloud base.

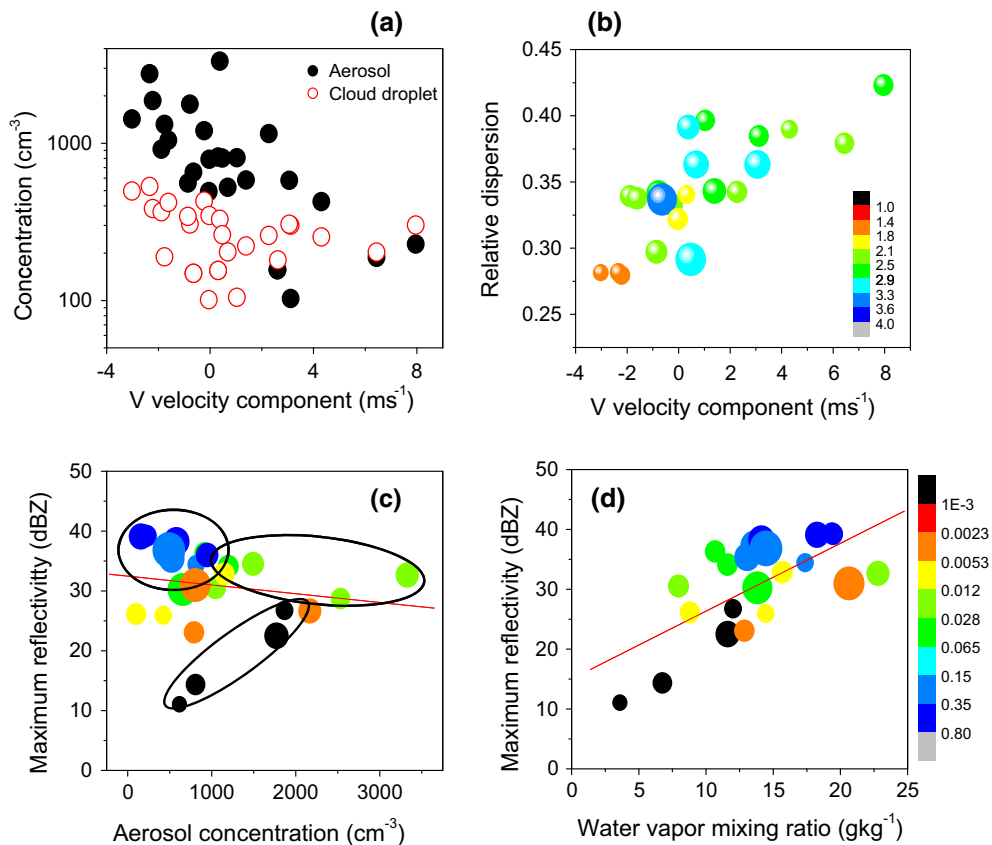The relative dispersion (ratio of spectral width and mean radius) averaged for 1 km above cloud base

Figure 6

The relationship between the boundary layer v component of wind and aerosol/cloud droplet number concentration (**a**), v component of wind and relative dispersion (**b** color is spectral width in μm and size of symbol is mean radius, averaged upto1 km above cloud base). Correlation between maximum reflectivity and aerosol concentration (**c**), maximum reflectivity and boundary layer water vapor mixing ratio (**d**). The rain rate is shown by color scale and mean radius by the size of the symbols in **c** and **d**

is shown in Fig. 6b. Relative dispersion also shows a strong dependence on the air mass origin. However, the spectral width and mean radius (indicated in the figure with color scaling and size of the symbols, respectively) have more complex relation with the air mass characteristics. The high relative dispersion is associated with maritime like observations (where the spectral width is moderately high). Low relative dispersion correspond to the cases that have a continental origin, having both low spectral width and low mean radius. However, largest spectral width and mean radius correspond to intermediate relative dispersion. These results confirm that the aerosol–cloud interactions (indirect effect and dispersion characteristics) derived from these observations are controlled by the dynamical conditions (wind direction) during the monsoon. Different sources of aerosol particle interact with cloud microphysics differently. Generally, wet monsoon has maritime aerosol source with lower number concentration but dry pre-monsoon has continental aerosol source (from north-west side) with high number concentration. Relative dispersion in monsoon clouds has significant variation as mentioned above and such information will be useful in numerical models where constant relative dispersion is typically used.

In situ measurements are used here to derive maximum reflectivity (dBZ) and average rain rate (mm h^{-1}) using cloud imaging probe (CIP) data in each flight observation and presented in Fig. 6c, d. Each point in this figure corresponds to a single flight observation (incloud). We investigated the

relationship between reflectivity and boundary layer mixing ratio as well as with boundary layer aerosol number concentration.

The observations can be classified into three categories (1: high aerosol and dry, 2: high aerosol and wet, 3: low aerosol and wet) depending on the moisture content and aerosol conditions. The high aerosol and dry regime is associated with widely varying maximum reflectivity (> 10 and < 25 dBZ) and lowest rain rates (black symbols). High aerosol and wet regime showed high (> 25 dBZ) reflectivity and moderate rain rate. Low aerosol and Wet (clean monsoon clouds) conditions have reflectivity > 30 dBZ and highest rain rate (blue symbols). Maximum reflectivity and rain rate show a clear linear relationship (positive correlation) with the boundary layer moisture content. This is further indicating that rain formation is also more closely associated with the boundary layer water vapor content.

The mean radius observed within 1 km of cloud base is also indicated in the Fig. 6c, d by the size of the symbols. Reflectivity is found to be maximum in the clouds having larger mean radius close to cloud base. Konwar et al. (2012) indicated the role of giant CCN in the formation of rain in these clouds. It may be noted that water vapor availability in the subcloud layer was indeed important in such situations for the raindrop formation. Rain rate is higher in clean and moist conditions and clouds have larger droplets (mean radius) near the cloud base, compared to other conditions mentioned earlier. Clouds with relatively smaller droplets near the base show lower reflectivity and no precipitation. Moderately large cloud droplets near the cloud base also contribute to moderate rain rates, possibly due to their role in collisions.

3.6. Vertical Structure of Parcel Buoyancy

A pseudo-adiabatic parcel model is utilized for the cases during pre-monsoon and monsoon conditions to obtain the profile of buoyancy and cumulative CAPE (cCAPE) of parcels ascending from the surface (Bera, Prabha, et al. 2016; Thomas et al. 2018). The parcel properties are displayed in Fig. 7. Upper panel shows parcel buoyancy and lower panel shows cCAPE. Cloud base region is marked by

oval shape in upper panel. It is important to notice that parcel buoyancy increases quickly as it rises above the cloud base region in case of the dry pre-monsoon clouds. This feature leads to sharp increase of cCAPE above the cloud base. On the other hand, parcel buoyancy does not change much with height in monsoon clouds and results in little increase of cCAPE above the cloud base. These distinct buoyancy profiles in pre-monsoon and monsoon conditions are due to the difference in moisture content above the boundary layer. Monsoon conditions characterize a significant moistening in the middle and upper atmosphere depending on its progression.

Usually pre-monsoon environment is drier above the boundary layer height which results in stronger environmental lapse rate and higher parcel buoyancy. On the other hand, monsoon environment is wet above the boundary layer (due to south-westerly wind) which results in lower ambient lapse rate and less parcel buoyancy. This thermodynamic feature of cloud parcels seems to impact microphysical structure of these clouds, discussed later. Another important aspect to be noted is that in the situations where subcloud parcel buoyancy is high, it is also high at elevated altitudes during the pre-monsoon environment. Good examples are for 28th May and 17th June cases. Meanwhile, 20th June shows that parcel buoyancy in the middle of the subcloud layer has increased and there is a smooth transition from subcloud layer to the cloud layer. The parcel model clearly shows that cloud base heights are relatively elevated in pre-monsoon cases and low during monsoon cases which was reported in earlier studies from aircraft observations (Prabha et al. 2011; Bera et al. 2016b).

3.7. Vertical Variation of Observed Microphysical Parameters

We now investigate the vertical variation of microphysical parameters such as cloud droplet number concentration (CDNC), mean radius (r_m), spectral width (σ) and relative dispersion (ε). It is to be noted that different flight observations are classified into three classes as PRE, MON1and MON2. The MON1 cases showed lowest CDNC (wet and clean
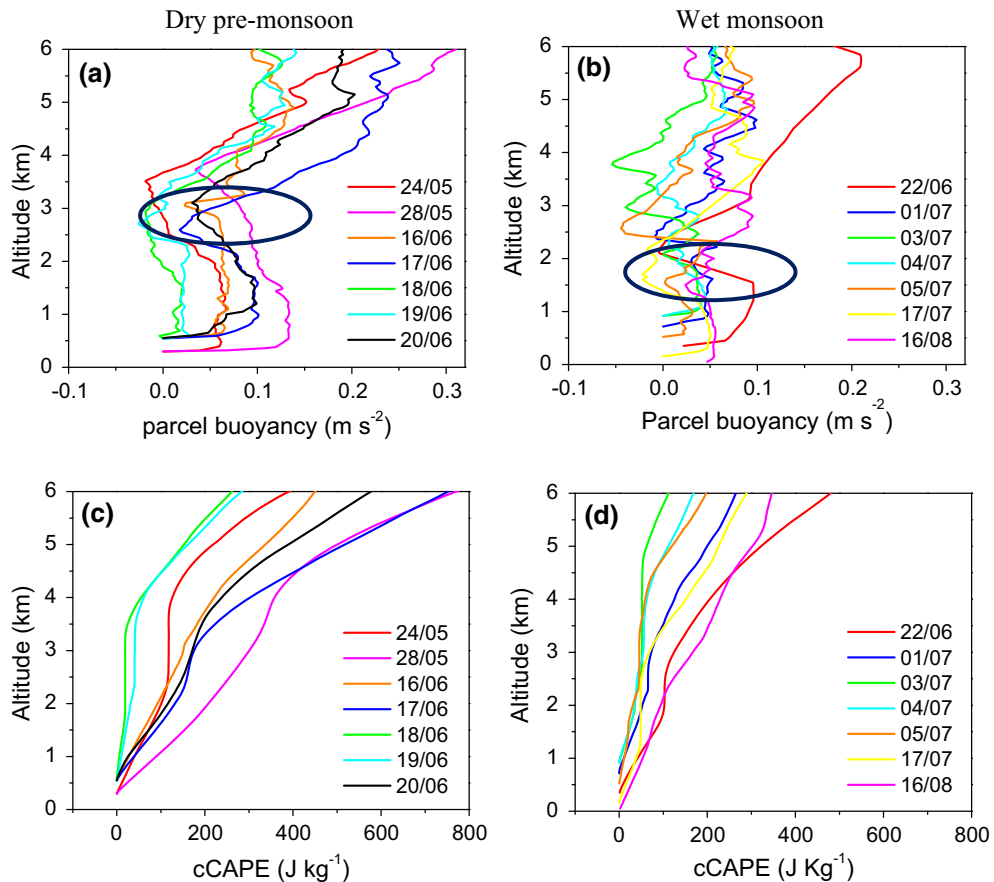
Figure 7
Vertical variation of parcel buoyancy and cCAPE during pre-monsoon (left) and monsoon environment (right). Circular ring in upper panel indicates region of cloud base

monsoon clouds) and the MON2 cases showed higher CDNC (> 200 cm^{-3}) correspond to wet and polluted monsoon clouds. In PRE case, mean CDNC is often greater than 300 cm^{-3}, corresponded to dry and highly polluted pre-monsoon clouds. Vertical variation of droplet number concentration shows distinct behavior in the dry and wet conditions (Fig. 8 top panel). In general, the dry conditions exhibit mean droplet number concentrations exceeding 300–400 cm^{-3} near the cloud base and observed to increase (by about 100 cm^{-3}) with height for few hundred meters just above cloud base and decrease thereafter. In the case of wet conditions, aerosol number concentrations are lower which produce the mean CDNC values also lower near the cloud base and typically do not show any increase with height.

The contrasting microphysical feature near to the cloud base is related to contrasting thermodynamic feature of cloud parcels as indicated in Fig. 7 where buoyancy increases linearly in pre-monsoon condition but nearly constant in monsoon environment. It is argued that higher parcel buoyancy and cCAPE in pre-monsoon environment provide additional droplet activation that increases number concentration above the cloud base. Standard deviation of droplet number concentration is presented by horizontal error bars and indicates higher variance in pre-monsoon clouds which may be attributed to droplet evaporation (by entrainment) and activation. Vertical variation of droplet mean radius is shown in the lower panel of Fig. 8. Relatively smaller droplet mean radii are observed in pre-monsoon clouds compared to
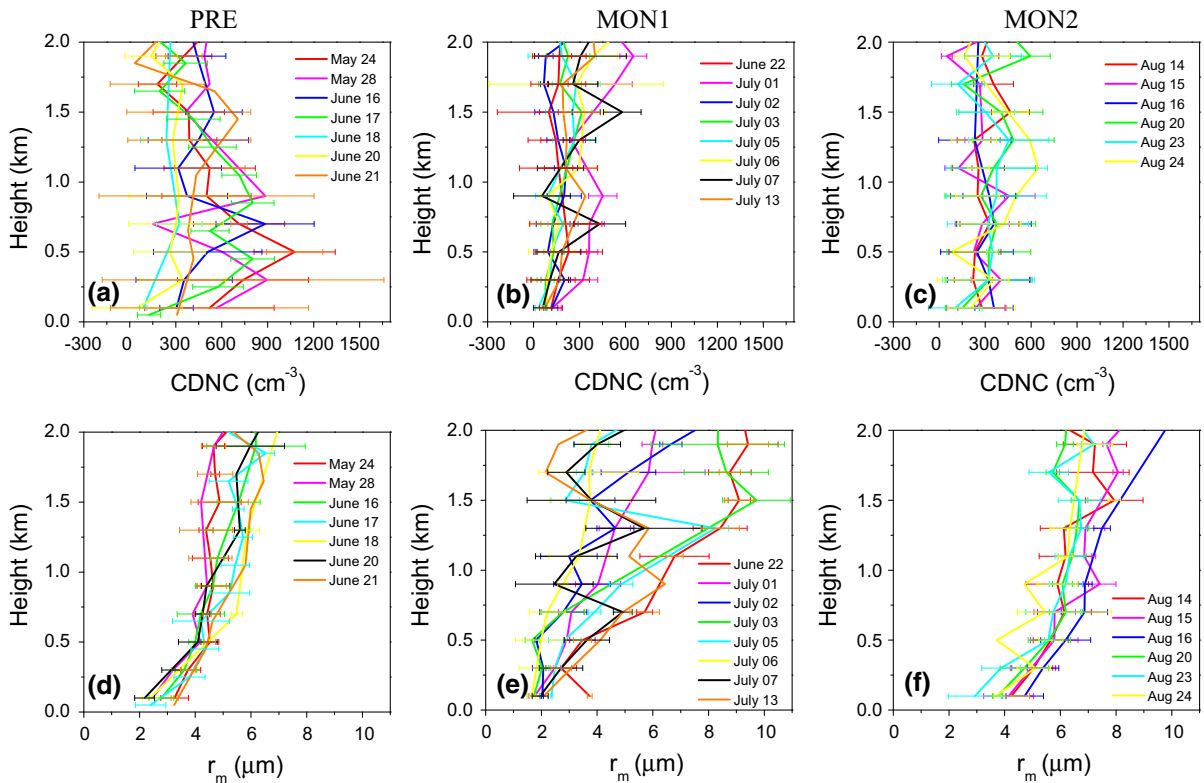
Figure 8
Vertical variation of droplet number concentration (upper panel) and mean radius (lower panel) averaged in 200 m vertical bins. Error bars represents standard deviation in each altitude level

monsoon clouds where larger droplets are present. Droplet radius increases with height due to condensational growth. Standard deviation of mean radius is comparable in all cases. It may also be noted that MON2 mean radius is higher than that of MON1 which is due to the fact that MON2 is possibly influenced by GCCN availability and higher moisture (Konwar et al. 2012). The vertical profiles of microphysical parameters are shown only up to 2 km above cloud base which is due to the fact that we have tried to connect boundary layer thermodynamics and cloud microphysics in the vicinity of the cloud base, which may be limited to 1–2 km and above that height, microphysics will be influenced by dynamical effects such as entrainment-mixing.

Droplet spectral width and relative dispersion is presented in Fig. 9. Spectral width generally increases with height for all cases except few premonsoon cases. However, the mean values of spectral width are different in different cases. For PRE cases it varies between 1–2 μm, for MON1 cases 1–3 μm and for MON2 cases 2–3 μm. Higher spectral widths in MON1 and MON2 cases are due to the presence of large droplets activated from GCCN and also due to collision–coalescence process. Typical behavior of relative dispersion in the pre-monsoon dry conditions shows maximum value (0.4–0.5) near the cloud base and a gradual decrease with height above. This is due to relatively constant spectral width variation with height, a competing effect of droplet evaporation and new activation. The spectral width remained constant but mean radius increases with height due to diffusional growth, which results in decreased relative dispersion with height. For monsoon clouds, relative dispersion is almost constant with height and is varying within a small range 0.3–0.6. This can be attributed to similar changes (increase with height) in mean radius and droplet spectral width and as a
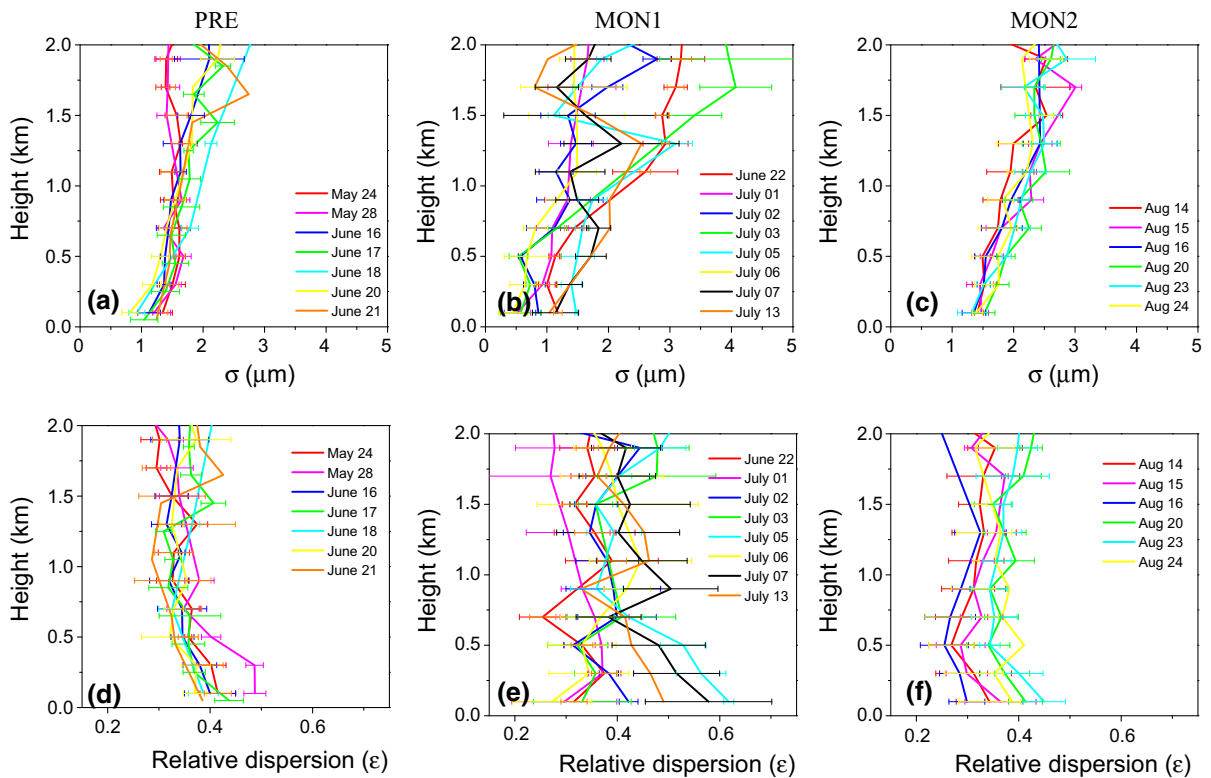
Figure 9
Vertical variation of droplet spectral width (upper panel) and relative dispersion (lower panel). Error bars represents standard deviation in each height level

results, ratio (relative dispersion) of these two remained almost constant with height. In the monsoon clouds with wet condition, the relative dispersion is relatively higher compared to dry premonsoon cases. The spectral broadening in monsoon clouds is explained with various processes and the incloud nucleation and droplet evaporation seem to be important in contributing to higher spectral width and the relative dispersion (Prabha et al. 2012).

3.8. Microphysics from Parcel Model

The results from CAIPEEX observations show that vertical variations of CDNC and droplet mean radius in pre-monsoon and monsoon clouds show contrasting characteristics. We hypothesized that parcel buoyancy and cCAPE have important role to determine vertical distribution of microphysical parameters for limited depth (1–2 km). To examine

this hypothesis, we carried out a 1-D parcel model run which includes microphysics of aerosol, droplet activation and diffusional growth. This is same cloud model as used before by Kucienska et al. (2010). We did not attempt to study chemistry of aerosol in this paper as there were no chemistry measurements done during the 2009 campaign. Our focus in this study is only on the warm phase of clouds and the ice processes and ice nuclei particle (INP) observations during the campaign are discussed in previous studies (Patade et al. 2015, 2016). The parcel model used here does not include ice microphysics, so only warm part of the cloud is studied.

Using two distinct thermodynamic soundings, one from pre-monsoon (June 16) and other from monsoon (June 22), we have illustrated vertical distribution of CDNC and mean radius at two CCN conditions (low CCN: 340 cm^{-3}, and high CCN: 980 cm^{-3}, typical during the campaign) and presented in Fig. 10. The
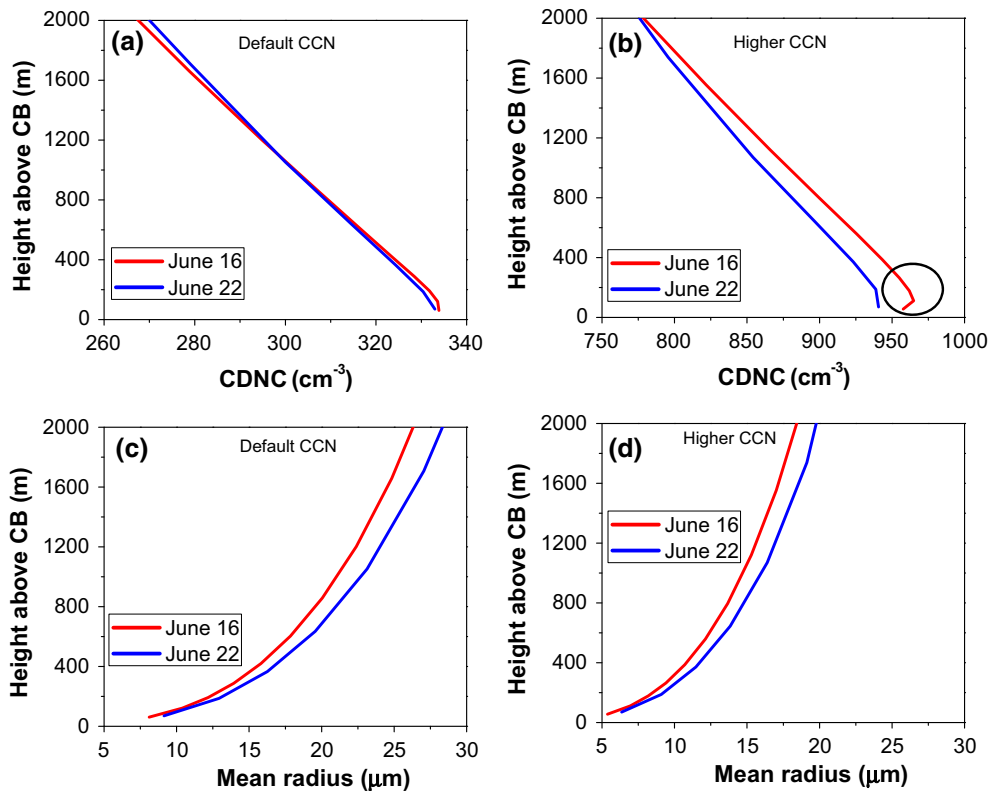
Figure 10
Vertical variation of CDNC and mean radius from parcel model

default (low) CCN is analogues to monsoon situation and higher CCN is likewise polluted pre-monsoon condition. It is interesting to see that a simple microphysical parcel model is capable of replicating similar features as found by in situ aircraft observations. At same CCN number concentration, pre-monsoon environment (16 June) produces higher droplet number for few hundred meters above the cloud base. For higher CCN situation, cloud parcel in pre-monsoon environment shows maximum droplet activation at an altitude of 200 m above the cloud base which is an observed feature during CAIPEEX where pre-monsoon clouds have highest droplet number at altitude few hundred (200–500) m above cloud base. It is also found from the parcel model that mean radius of droplets may vary at same CCN condition if environmental conditions are different.

Pre-monsoon environment is relatively dry and produces slightly smaller droplets as compared to monsoon cloud at all heights above cloud base which is purely due to less diffusional growth in dry environment. It is obvious that absolute values of mean radius are very high in parcel model as compared to observation which is a true fact because the parcel model does not include the effect of dry air entrainment which decreases droplet size by evaporation. Another important process that may reduce droplet mean radius in real clouds is the entrainment of fresh CCN through lateral cloud edges and incloud activation of small droplets (Derksen et al. 2009). Incloud activation of fresh CCN in monsoon clouds has been reported in many previous studies (Prabha et al. 2011; Konwar et al. 2015; Bera, Pandithurai, et al. 2016). In higher CCN case, dry pre-monsoon cloud produces more droplet activation above cloud base (marked by a circle) which is enhanced due to thermodynamic effect.
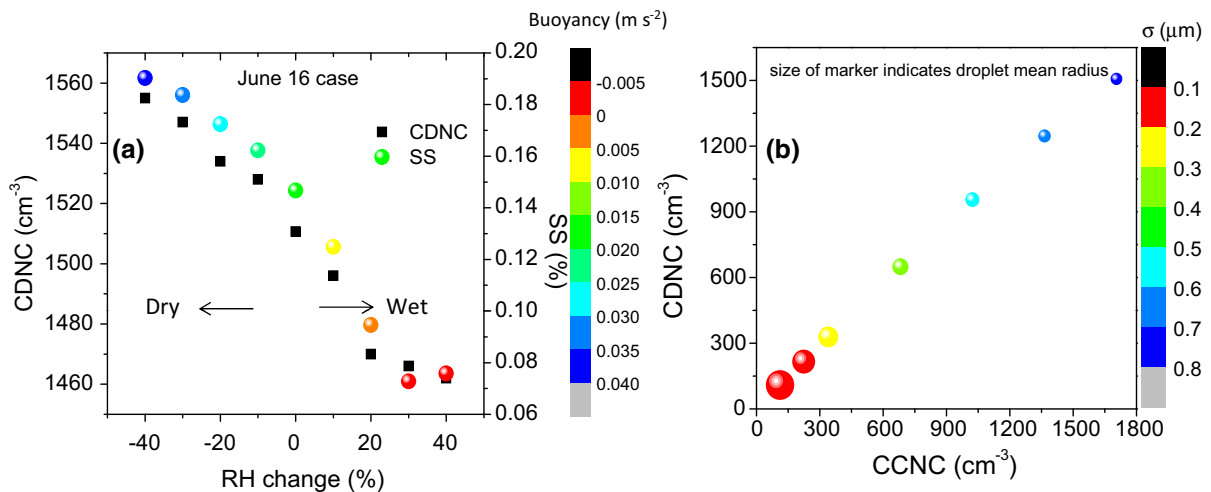
Figure 11

Model sensitivity to **a** environmental RH and **b** CCN concentration. Variation of cloud droplet number concentration (CDNC), supersaturation at the cloud base and buoyancy (m s^{-2}, in color) with changes in environmental RH are illustrated in **a**. Relationship between CCNC and CDNC is illustrated in **b**. Color indicates the droplet spectral width and size of the symbol indicates mean radius of droplets at the cloud base

3.8.1 Thermodynamic Effect from Parcel Model

To understand further about the thermodynamic effect on microphysics we performed several simulations by increasing/decreasing RH (up to 40% higher or lower than the default case) of the environment and keeping the other parameters same as default. Our intention here is to see the effect of the environmental moisture on the droplet spectrum independently. This kind of analysis is not possible from observations as both aerosol and moisture conditions changed from place to place as monsoon progressed. Sensitivity to environmental RH is investigated on the pre-monsoon (higher CCN) cloud case. The changes in droplet number concentration, mean radius, parcel buoyancy and supersaturation at cloud base are presented in Fig. 11a. Positive RH conditions have lower buoyancy and lower SS at cloud base as seen in the observations (monsoon wet cases) and RH deficit cases have greater SS and buoyancy inside the cloud. This higher SS is attributed to increase in buoyancy, which explains increasing number concentration (for 200 m above cloud base) in the dry polluted case as shown in Fig. 10b. These results give convincing evidence that the initial increase in droplet number concentration above cloud base as seen in several of our observations can be attributed to the enhancement of supersaturation due to the buoyancy effects. The variation in RH can cause up to 10% increase in the number concentration in the presented case. Although, these effects are important in both dry and wet conditions, the impact during the polluted and dry condition is large due to the presence of more CCN, which gets activated slightly above cloud base.

3.8.2 Aerosol Effect from Parcel Model

During pre-monsoon to monsoon transition, we encounter significant changes in aerosol (or CCN) concentration near the cloud base. To investigate the impact of increase in CCN for a fixed thermodynamic condition, we carried out CCNC sensitivity case studies by varying CCNC from 50 to 1700 cm^{-3}. The cloud microphysical changes noticed from the simulations are presented in Fig. 11b. CDNC and CCNC are linearly related but droplet mean radius is inversely related which is similar to the Twomey effect (Twomey 1977). Spectral width is very narrow in low CCN condition and gets broadened when CCN concentration is higher. So, relative dispersion (ratio of spectral width and mean radius) increases with increasing CCNC.

In case of CAIPEEX observation, due to its strategy as the base station moved depending on the progression of monsoon over land areas, it is not possible to analyze the indirect effect for specific thermodynamic condition or vice versa. We used a parcel model to show that there can be at least 10% variation in the cloud droplet number concentrations due to the supersaturation changes attributing to different thermodynamics (see Fig. 11a describing this aspect). Meanwhile, the aerosol cloud interaction with aerosol sensitivity is presented in Fig. 11b. The parcel model gives a linear increase in droplet number concentrations with increase in CCN. Droplet sizes have decreased and spectral width has increased in such a scenario. Figure 11b is addressing the aerosol indirect effect while holding the thermodynamic conditions constant.

4. Discussion and Conclusions

Findings from the observations conducted during CAIPEEX -2009 are presented in this study with a main focus on the thermodynamic effects on cloud microphysics and relative importance of aerosol. Observations were conducted at different locations as monsoon progressed inland. The overall picture emerges that cloud–aerosol interaction during the experiment was largely controlled by availability of boundary layer water vapor and air mass origin. Overall three classes of observations are presented, based on the humidity and aerosol, which showed distinct vertical variation of microphysical variables.

Pre-monsoon thermodynamics is characterized by higher buoyancy and cCAPE compared to monsoon environment. Buoyancy increases sharply just above the cloud base in pre-monsoon cases. Airborne observations indicated $2\text{--}3\ \text{m s}^{-1}$ incloud mean updrafts with significant spatial variation (error bars) which indicates high variance of the vertical velocity ($w^{'2}$) and thus high turbulence energy. Clouds during the monsoon are significantly entrained and were found to be less adiabatic than pre-monsoon clouds, noticed by the negative relationship between vapor mixing ratio and adiabatic fraction. On the other hand, the entrainment rate in the lower part of the clouds (up to 2 km height) did not show a noticeable

relationship with the boundary layer water vapor, but showed a weak relation with aerosol number concentration. Less polluted monsoon clouds have slightly higher entrainment rate which helps in diluting the clouds. Although, there can be other dynamical factors that may result in less adiabatic monsoon clouds, which are not explored here.

It can be noted that the aerosol and droplet number concentration decreased with intrusion of marine air mass during the progression of monsoon. Relative dispersion increased with more maritime air mass, indicating that relative contribution from droplet spectral width is dominating compared to mean radius of droplets. We then investigated the root cause of vertical variation of droplet number concentration. In pre-monsoon clouds, droplet number concentration showed a peak at few height levels above cloud base and then it decreases further. This peak is attributed to enhancement of the positive buoyancy and supersaturation. This extra supersaturation available in the pre-monsoon clouds indeed activated those small particles that could not get activated at the cloud base. In the monsoon conditions (wet), the availability of few CCN particles and larger droplets at cloud base facilitate raindrop formation at lower altitudes.

The comparison of droplet spectra from pre-monsoon and monsoon clouds showed distinct behavior (Prabha et al. 2012) with large number concentration and narrow spectra in pre-monsoon clouds, while monsoon clouds had wider spectra and less droplet number concentrations. The present study argues that the higher droplet number concentration and narrower spectra noted in the lower part of the pre-monsoon clouds are indeed forced by the subcloud buoyancy, which introduced enhanced vertical velocities and additional supersaturation required for activation of more aerosol particles. This process can change droplet number concentration to 10% for a change in RH $\pm$ 40% corresponding to a supersaturation change of up to 0.1% near the cloud base in the pre-monsoon conditions. This is indeed maintaining the near linear variation in mean radius with almost no change in spectral width and nearly linear decrease in relative dispersion.

The underlining point is that subcloud-layer-induced buoyancy does play an important role in the

initial few hundred meters above cloud base which results in higher vertical velocities and higher supersaturation compared to monsoon case. The high supersaturation facilitates activation of more CCN and droplet formation within a few hundred meters above the cloud base in pre-monsoon environment. Entrainment rate in these clouds is lower compared to monsoon clouds. These differences may lead to more adiabatic core in the pre-monsoon clouds, compared to the monsoon clouds. Many flight observations conducted over different locations and several parcel model simulations are utilized to illustrate this point. Observations could not be conducted in similar thermodynamic environments as desired and thus the parcel model sensitivity results are presented in the study. Numerical simulations support the observational findings as illustrated.

Acknowledgements

REFERENCES

Ackerman, A. S., Kirkpatrick, K. P., Stevens, D. E., & Toon, O. B. (2004). The impact of humidity above stratiform clouds on indirect aerosol climate forcing. *Nature, 432,* 1014–1017. https://doi.org/10.1038/nature03174.

Albrecht, B. (1989). Aerosols, cloud microphysics, and fractional cloudiness. *Science, 245,* 1227–1230. https://doi.org/10.1126/science.245.4923.1227.

Andrea, M. O., Rosenfeld, D., Artaxo, P., Costa, A. A., Frank, G. P., Longo, K. M., et al. (2004). Smoking rain clouds over Amazon. *Science, 303,* 1337–1342.

Bera, S., Pandithurai, G., & Prabha, T. V. (2016a). Entrainment and droplet spectral characteristics in convective clouds during transition to monsoon. *Atmospheric Science Letters, 17,* 286–293. https://doi.org/10.1002/asl.657.

Bera, S., Prabha, T. V., & Grabowski, W. W. (2016b). Observations of monsoon convective cloud microphysics over India and role of entrainment-mixing. *Journal of Geophysical Research: Atmospheres, 121,* 9767–9788. https://doi.org/10.1002/2016jd025133.

Blyth, A., Cooper, W. A., & Jensen, J. B. (1988). A study of the source of entrained air in Montana cumuli. *Journal of Atmospheric Science, 45,* 3944–3964. https://doi.org/10.1175/1520-0469(1988)045<3944:ASOTSO>2.0.CO;2.

Böing, S. J., Jonker, H. J. J., Nawara, W. A., & Siebesma, A. P. (2014). On the deceiving aspects of mixing diagrams of deep cumulus convection. *Journal of the Atmospheric Sciences, 71,* 56–68.

Derksen, J. W. B., Roelofs, G.-J. H., & Rockmann, T. (2009). Influence of entrainment of CCN on microphysical properties of warm cumulus. *Atmospheric Chemistry and Physics, 9,* 6005–6015.

Fan, J., Rosenfeld, D., Zhang, Y., Giangrande, S. E., Li, Z., Machado, L. A. T., et al. (2018). Substantial convection and precipitation enhancements by ultrafine aerosol particles. *Science, 359*(6374), 411–418. https://doi.org/10.1126/science.aan8461.

Gayatri, K., Patade, S., & Prabha, T. V. (2017). Aerosol–Cloud interaction in deep convective clouds over the Indian Peninsula using spectral (bin) microphysics. *Journal of Atmospheric Sciences, 74,* 3145–3166. https://doi.org/10.1175/jas-d-17-0034.1.

Gerber, H., Frick, G., Jensen, J., & Hudson, J. (2008). Entrainment, mixing, and microphysics in trade-wind cumulus. *Journal of the Meteorological Society of Japan, 86A,* 87–106.

Jensen, J. B., Austin, P. H., Baker, M. B., & Blyth, A. M. (1985). Turbulent mixing, spectral evolution and dynamics in a warm cumulus cloud. *Journal of the Atmospheric Sciences, 42,* 173–192.

Jensen, J. B., & Baker, M. B. (1989). A simple model of droplet spectral evolution during turbulent mixing. *Journal of the Atmospheric Sciences, 46,* 2812–2829.

Khain, A. P. (2009). Notes on state-of-the-art investigations of aerosol effects on precipitation: A critical review. *Environmental Research Letters, 4,* 015004. https://doi.org/10.1088/1748-9326/4/1/015004.

Khain, A. P., Roseenfeld, D., & Pokrovsky, A. (2005). Aerosol impact on the dynamics and microphysics of deep convective clouds. *Quarterly Journal of the Royal Meteorological Society, 131,* 2639–2663. https://doi.org/10.1256/qj.04.62.

Konwar, M., Maheskumar, R. S., Kulkarni, J. R., Freud, E., Goswami, B. N., & Rosenfeld, D. (2012). Aerosol control on depth of warm rain in convective clouds. *Journal of Geophysical Research: Atmospheres, 117,* D13204. https://doi.org/10.1029/2012jd017585.

Konwar, M., Panicker, A. S., Axisa, D., & Prabha, T. V. (2015). Near-cloud aerosols in monsoon environment and its impact on radiative forcing. *Journal of Geophysical Research, 120,* 1445–1457.

Kucieńska, B., Montero-Martínez, G., & García-García, F. (2010). A simulation of the influence of organic and inorganic pollutants on the formation and development of warm clouds over Mexico City. *Atmospheric Research, 95,* 487–495.

Kulkarni, J. R., Maheshkumar, R. S., Morwal, S. B., Padma kumara, B., Konwar, M., Deshpade, C. G., et al. (2012). Cloud aerosol interaction and precipitation enhancement experiment (CAIPEEX): overview and preliminary results. *Current Science, 102,* 413–425.

Li, Z., Niu, F., Fan, J., Liu, Y., Rosenfeld, D., & Ding, Y. (2011). Long-term impacts of aerosols on the vertical development of clouds and precipitation. *Nature Geoscience, 4,* 888–894.

Lu, M. L., Feingold, G., Jonsson, H. H., Chuang, P. Y., Gates, H., Flagan, R. C., et al. (2008). Aerosol–cloud relationship in continental shallow clouds. *Journal of Geophysical Research: Atmospheres, 113,* D15201. https://doi.org/10.1029/2007JD009354.

Lu, C., Liu, Y., Yum, S. S., Niu, S., & Endo, S. (2012). A new approach for estimating entrainment rate in cumulus clouds. *Geophysical Research Letters, 39,* L04802.

Mechem, D. B., Yuter, S. E., & de Szoeke, S. P. (2012). Thermodynamic and aerosol controls in southeast Pacific stratocumulus. *Journal of Atmospheric Science, 69,* 1250–1266. https://doi.org/10.1175/jas-d-11-0165.1.

Miles, N. L., Verlinde, J., & Clothiaux, E. E. (2000). Cloud droplet size distributions in lowlevel stratiform clouds. *Journal of Atmospheric Science, 57,* 295–311.

Morrison, H., & Grabowski, W. W. (2007). Comparison of bulk and binwarm-rain microphysics models using a kinematic framework. *Journal of the Atmospheric Sciences, 64,* 2839–2861.

Murugavel, P., Malap, N., Balaji, B., Mehajan, R. K., & Prabha, T. V. (2017). Precipitable water as a predictor of LCL height. *Theoretical and Applied Climatology, 130,* 467.

Nair, S., Sanjay, J., Pandithurai, G., Maheskumar, R. S., & Kulkarni, J. R. (2012). On the parameterization of cloud droplet effective radius using CAIPEEX aircraft observations for warm clouds in India. *Atmospheric Research, 108,* 104–114. https://doi.org/10.1016/j.atmosres.2012.02.002.

Paluch, I. R. (1979). The entrainment mechanism in Colorado cumuli. *Journal of Atmospheric Science, 36,* 2467–2478.

Pandithurai, G., Dipu, S., Prabha, T. V., Maheshkumar, R. S., Kulkarni, J. R., & Goswami, B. N. (2012). Aerosol effect on droplet spectral dispersion in warm continental cumuli. *Journal of Geophysical Research: Atmospheres, 117*(1–15), D16202. https://doi.org/10.1029/2011jd016532.

Patade, S., Prabha, T. V., Axisa, D., Gayatri, K., & Heymsfield, A. (2015). Particle size distribution properties in mixed-phase monsoon clouds from in situ measurements during CAIPEEX. *Journal of Geophysical Research: Atmospheres, 120,* 10418–10440.

Patade, S., Shete, S., Malap, N., Kulkarni, G., & Prabha, T. V. (2016). Observational and simulated cloud microphysical features of rain formation in the mixed phase clouds observed during CAIPEEX. *Atmospheric Research, 169,* 32–45.

Prabha, T. V., Khain, A., Maheshkumar, R. S., Pandithurai, G., Kulkarni, J. R., Konwar, M., et al. (2011). Microphysics of pre-monsoon and monsoon clouds as seen from in situ measurements during CAIPEEX. *Journal of Atmospheric Science, 68,* 1882–1901.

Prabha, T. V., Patade, S., Pandithurai, G., Khain, A., Axisa, D., Pradeep-Kumar, P., et al. (2012). Spectral width of premonsoon and monsoon clouds over Indo-Gangetic valley. *Journal of*

Geophysical Research, 117, D20205. https://doi.org/10.1029/2011jd016837.

Raga, G. R., Jensen, J. B., & Baker, M. B. (1990). Characteristics of cumulus band clouds off the coast of Hawaii. *Journal of Atmospheric Science, 47,* 338–356.

Rangno, A. L., & Hobbs, P. V. (2005). Microstructures and precipitation development in cumulus and small cumulonimbus clouds over the warm pool of the tropical Pacific Ocean. *Quarterly Journal of the Royal Meteorological Society, 131,* 639–673.

Rosenfeld, D., Lohmann, U., Raga, G. B., O'Dowd, C. D., Kulmala, M., Fuzzi, S., et al. (2008). Flood or drought: How do aerosols affect precipitation? *Science, 321*(5894), 1309–1313.

Siebesma, A. P., et al. (2003). A large-eddy simulation intercomparison study of shallow cumulus convection. *Journal of the Atmospheric Sciences, 60,* 1202–1219.

Thomas, L., Malap, N., Grabowski, W. W., Dani, K., & Prabhakran, T. V. (2018). Convective environment in pre-monsoon and monsoon conditions over the Indian subcontinent: the impact of surface forcing. *Atmospheric Chemistry and Physics Discussions.* https://doi.org/10.5194/acp-2018-1.

Tölle, M. H., & Krueger, S. K. (2014). Effects of entrainment and mixing on droplet size distributions in warm cumulus clouds. *Journal of Advances in Modeling Earth Systems, 6,* 281–299. https://doi.org/10.1002/2012ms000209.

Twomey, S. (1977). The influence of the pollution in the shortwave albedo of clouds. *Journal of the Atmospheric Sciences, 34,* 1149–1152. https://doi.org/10.1175/1520-0469(1977)034<1149:TIOPOT>2.0.CO;2.

Wang, S., Wang, Q., & Feingold, G. (2003). Turbulence, condensation, and liquid water transport in numerically simulated non-precipitating stratocumulus clouds. *Journal of the Atmospheric Sciences, 60,* 262–278. https://doi.org/10.1175/1520-0469(2003)060<0262:tcalwt>2.0.co;2.

Warner, J. (1969). The microstructure of cumulus cloud. Part I. General features of the droplet spectrum. *Journal of the Atmospheric Sciences, 26,* 1049–1059.

Warren, S. G., Hahn, C. J., London, J., Chervine, R. M., & Jenne, R. L. (1986). Global distribution of total cloud cover and cloud type amounts over land. NCAR Tech. Note NCAR/TN-273 + STR, 29 pp.

Xue, H., & Feingold, G. (2006). Large-eddy simulations of trade wind cumuli: Investigation of aerosol indirect effects. *Journal of the Atmospheric Sciences, 63,* 1605–1622. https://doi.org/10.1175/jas3706.1.